

Variational Inference with Latent Space Quantization for Adversarial Resilience

Vinay Kyatham, Prathosh A. P.*, Deepak Mishra*, and Tarun Kumar Yadav
 Indian Institute of Technology Delhi
 New Delhi, India
 karunakyatham@gmail.com

Dheeraj Mundhra
 SigTuple Technologies
 Bangalore, India

Abstract

Despite their tremendous success in modelling high-dimensional data manifolds, deep neural networks suffer from the threat of adversarial attacks - Existence of perceptually valid input-like samples obtained through careful perturbations that leads to degradation in the performance of underlying model. Major concerns with existing defense mechanisms include non-generalizability across different attacks, models and large inference time. In this paper, we propose a generalized defense mechanism capitalizing on the expressive power of regularized latent space based generative models. We design an adversarial filter, devoid of access to classifier and adversaries, which makes it usable in tandem with any classifier. The basic idea is to learn a Lipschitz constrained mapping from the data manifold, incorporating adversarial perturbations, to a quantized latent space and re-map it to the true data manifold. Specifically, we simultaneously auto-encode the data manifold and its perturbations implicitly through the perturbations of the regularized and quantized generative latent space, realized using variational inference. We demonstrate the efficacy of the proposed formulation in providing the resilience against multiple attack types (Black and white box) and methods, while being almost real-time. Our experiments show that the proposed method surpasses the state-of-the-art techniques in several cases.

1. Introduction

Deep neural networks have shown tremendous success in various computer vision tasks. One of the primary factors contributing to their success is the availability of abundant data. This generally leads to an incomplete exploration of

data space with the available training set, which in-turn results in loopholes in the data manifold [7, 31]. The so-called adversarial attacks exploit these gaps in the data manifold, unexplored by the classifier, and leads to the failure of otherwise successful networks. Commonly, this unexplored subspace, can be called as *adversarial subspace*, contains adversarial samples generated using perturbation of original training samples with carefully designed synthetic noise [10, 36, 25, 4, 21]. This is an important concern not only from a point of security but also from a generalization perspective [38]. In rest of the section, we will present an overview of the existing adversarial attacks, defense mechanisms along with a motivation for our work.

1.1. Adversarial attacks - General principles

An adversarial sample is obtained by perturbing the input sample with a small amount such that perceptual quality is unaltered but the class label is changed under a classifier. Formally, let $\mathbf{x} \in \mathbb{R}^M$ denote a sample from the natural data manifold and $\mathbf{x}' = \mathbf{x} + \delta$, denote a perturbation on \mathbf{x} with $\delta \in \mathcal{S}$, $\mathcal{S} \subseteq \mathbb{R}^M$ being the space of all possible perturbations. Under a given distance metric \mathcal{D} and a classification scheme $h(\mathbf{x})$, the sample \mathbf{x}' is called an adversarial example for \mathbf{x} if $\mathcal{D}(\mathbf{x}, \mathbf{x}') \leq \epsilon$ and $h(\mathbf{x}) \neq h(\mathbf{x}')$. A large body of attacks consider a l_p -norm based \mathcal{D} , with l_2 and l_∞ norms being the significant ones, and solve an optimization problem on the loss function of $h(\mathbf{x})$ to obtain the desired δ . Attacks can be targeted so that the classifier is misguided to a specific class or non-targeted so that it outputs an arbitrary class different from the original class. Further categorization of adversarial attacks is based on the level of access the attacker has about the classification and defense scheme.

1. Black-box attacks - The attacker neither has the access to the original classifier nor the defense scheme, rather he has to generate adversarial examples on a substitute classifier [27]. It has been found that often attacks

*Equal contribution.

generated on these substitutes generalize on the original classifier as well [36].

2. White-box attacks - In this case, it is assumed that the attacker has access to the original classifier and the defense mechanism. In other words, the adversarial examples can be generated by computing gradients over both the original classifier and the defense networks.

1.2. Attack methods

There is a gamut of literature on creating adversarial attacks [36, 10, 17, 25, 4, 28, 37, 16]. We choose Fast Gradient Sign Method (FGSM) [8], Basic Iterative method [16], Deepfool Attack [25] and Carlini-Wagner (CW) attack [4] since they cover a good breadth of the class of attacks.

Fast Gradient Sign Method (FGSM): Goodfellow et al. proposed a fast and simple method that relies on taking a first-order Taylor’s series approximation on the loss term [10]. This performs a one step gradient update along the direction of sign of gradient at each pixel to make the sample adversarial. Let $L(\mathbf{x}, y)$ be the loss function for image \mathbf{x} with correct label y . FGSM computes the perturbation δ as:

$$\delta = \epsilon \cdot \text{sign}(\nabla_{\mathbf{x}}(L(\mathbf{x}, y))) \quad (1)$$

where ϵ is a hyper-parameter that controls the size of the perturbation.

Basic Iterative Method (BIM): Kurakin et al. extended FGSM by applying multiple small steps α in the direction of gradient instead of one ϵ step [17][22]. In each iteration the pixel values are clipped by same ϵ to avoid large changes. Formally, BIM finds an adversarial example as follows:

$$\mathbf{x}'_{N+1} = \mathbf{x}'_N + \text{Clip}_{\epsilon}(\alpha \cdot \text{sign}(\nabla_{\mathbf{x}}L(\mathbf{x}'_N, y))) \quad (2)$$

Here \mathbf{x}'_N is the adversarial sample obtained after N iterations started with $\mathbf{x}'_0 = \mathbf{x}$.

Deepfool Attack: Deepfool [24] is also an iterative attack which computes the adversarial perturbation through an orthogonal projection of the sample on the decision boundary. If $h(x)$ is the classifier, w being its decision boundary, then the Deepfool method computes the perturbation δ as follows

$$\delta = -\frac{h(\mathbf{x})}{\|w\|_2} w \quad (3)$$

Carlini-Wagner Attack: CW is an optimization based attack that used logits-based objective function instead of commonly used cross-entropy loss [3]. The perturbation is found by optimizing the function:

$$\begin{aligned} \min_{\delta \in \mathbb{R}^n} \mathcal{D}(\mathbf{x}, \mathbf{x} + \delta) + c \cdot h(\mathbf{x} + \delta) \\ \text{s.t. } \mathbf{x} + \delta \in [0, 1]^n \end{aligned} \quad (4)$$

where \mathcal{D} is a distance metric (most often l_0 , l_2 , or l_{∞}), c is a suitably chosen constant and $h(\mathbf{x}') \leq 0$ if and only if classifier misclassifies \mathbf{x}' . CW is one of the most powerful attacks till date in the sense that it breaks many of the defense strategies [4].

2. Prior art on defense mechanisms

A large number of defense mechanisms to diminish the effect of adversarial attacks is available [8, 30, 14, 35, 33, 23, 21, 29]. Broadly, these can be divided into the following categories -

1. Classifier retraining - In this class of methods the basic idea is to retrain the original classifier with the adversarial examples so that the decision boundary is re-adjusted to accommodate the adversarial examples.
2. Modified training - Here the idea is to tweak the training procedure and/or the training examples of the classifier so that the learned decision boundary is robust to adversarial examples.
3. Adversarial filtering - This class of methods attempt to filter the adversarial noise either by manifold projection or generative models. The advantage of these over the previous two is that they are non-obtrusive in the sense that do not need the access to the original classifier.

Adversarial Retraining

A natural way to make the classifier robust against the adversaries is to retrain the classifier using the adversarial examples [8, 36]. While this is a simple and promising method for defense, in its naive formulation, it is shown to be ineffective towards black-box attacks [11] since the extent of retraining depends upon the quality of the generated adversaries [6, 32]. Several improvisations of adversarial retraining have been proposed. Madry et al. coupled the adversarial generation with the classifier training by solving a saddle-point problem using a projected gradient method [21]. This method is showed to be robust against many first-order l_{∞} -bounded adversaries but not against other attacks such as Deepfool and CW [37]. Sinha et. al. [34] claims certifiable adversarial robustness on MNIST through retraining by perturbing the underlying data distribution in a Wasserstein ball. In [37], an adversarial training procedure is proposed through augmentation of training data with perturbations transferred from other models.

Modified Training

These methods tweak the training procedure to make the decision boundary robust. For example, [29] uses the principle of distillation during neural network training to extract

knowledge about training points and gradients and use this knowledge to re-train the classifier. Guo et al. [13] applies several transformations such as bit-depth reduction, JPEG compression, variance minimization, and image quilting on the input images to augment the training set and claim resilience against adversarial attacks. Xiao et al. [39] mention that induction of sparsity in the weight space and stability in the ReLU non-linearity results in robustness. Dhillon et al. [5] induces stochasticity into the activation of the networks to defend against adversarial examples. In [40], a randomization layer is added before the input of the neural network as a defense strategy. However, Anish et al [2] demonstrate that most of these defenses are vulnerable because they capitalize on obfuscated gradients that can be mitigated.

Adversarial filtering

These defenses do not modify the classifier and also not require knowledge of the process generating adversarial examples. The basic idea is to modify the adversarial example with pre-processing to make it non-adversarial. For example, MagNet [23] trains a collection of detector networks that differentiate between normal and adversarial examples. It also includes a reformer network (one or collection of auto-encoders) to push adversarial examples close to data manifold. A recent strategy called Defense-GAN [30] trains a generative adversarial network (GAN) [9] only on legitimate examples and uses it to denoise adversarial examples. At the time of inference, they find images from the range of generator that are near the input image but lie on legitimate data manifold. This requires L iterations of back propagation for R random Initialization to find the nearest legitimate image, typical values of L is 200 and R is 10. Other GAN based defences, for example, PixelDefend [35] and APE-GAN [33], perform image-to-image translation to convert an adversarial image into a legitimate image.

2.1. Problem setting and our contributions

As mentioned, while the existing defense mechanisms have their own merits, each of them suffer from disadvantages. Adversarial retraining methods need access to the adversarial samples and are often prone to change in the attack type. For instance, a classifier adversarially retrained on an l_∞ attack does not generalize to a l_2 attack. Methods that modify the training procedure are found to be easily attackable by gradient-based first-order techniques since most of them are feed-forward neural network. Although generative model-based defenses such as Defense-GAN are less vulnerable, they demand a very large inference time and compute capacity due to the latent-space search. To alleviate aforementioned issues, in this paper, we propose a defense mechanism based on quantized latent variable generative autoencoders. Our contributions are enlisted below:

1. Propose a latent variable generative model based defense mechanism devoid of access to classifier and adversaries.
2. Auto-encoding the data space with perturbation such that an inverse mapping from the latent to the legitimate data space is obtained.
3. Construction of a Lipschitz constrained latent encoder that preserves the distances under a metric spaces on the latent and the data manifolds.
4. Constraining the latent space to follow a known distribution so that stochastic exploration of the latent neighbourhood corresponding to the data neighborhood is possible.
5. Use of dual decoders with a quantization on the latent space so that a large neighbourhood around a data sample is explored and easily remapped back to the data point.
6. Use of the Lipschitz constrained encoder and discrete decoder on the quantized latent space during inference so that the overall defense model is non-vulnerable to gradient-based white-box attacks.

3. Proposed Method

3.1. Motivation

In many previous works it is hypothesized that the adversarial examples fall off the data manifold [19, 30]. This suggests that a defense model could be potentially built by replacing an adversarial example with the nearest correctly-classified sample from the data manifold. However, searching in high-dimensional data manifolds is expensive, not generalizable and moreover, it has been found that the adversarial examples might fall on the data manifold too [7]. Thus, a better approach could be to project the data manifold onto an explorable compact generative latent space and remap the latent codes back to the legitimate data. If the latent space projector is made to be Lipschitz constrained and compact, then one can hope that adversarial examples adhere to a latent code that is invertable to the legitimate data.

3.2. Lipschitz constrained latent transformation

Let $f(\mathbf{x}) : \mathbb{R}^N \rightarrow \mathbb{R}^M$ represent a function which maps a data point \mathbf{x} of dimension N to latent vector \mathbf{z} of dimension M such that $M < N$. For a linear f , the adversarial perturbation, δ on \mathbf{x} will result an equivalent perturbation δ_z on \mathbf{z} such that $\delta_z = f(\delta)$. If f is constrained to K -Lipschitz, then bounded perturbations in \mathbf{x} results in a controllable bounded perturbation in \mathbf{z} as affirmed by the following proposition.

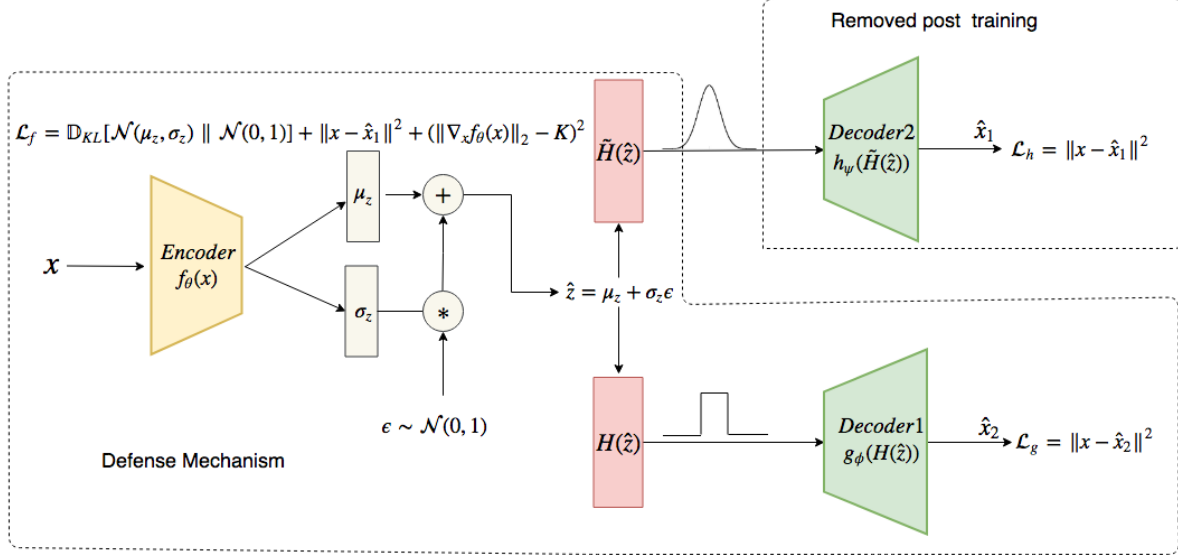


Figure 1. Proposed LQ-VAE - A Lipschitz constrained encoder (L_f) encodes the input image into a latent space quantized by the function H which is explored through a stochastic perturbation (ϵ). During inference, Decoder1 maps the quantized latent codes generated by the adversarial images back to the image space. Training is done **only on real data samples** by using an approximate differentiable version of Decoder1 (i.e. Decoder2).

Proposition 1: If f is K -Lipschitz and δ is bounded by c , δ_z will be bounded by $c.K$.

Proof: given f is K -Lipschitz,

$$|f(\mathbf{x} + \delta) - f(\mathbf{x})| \leq K \cdot \|\mathbf{x} + \delta - \mathbf{x}\| \quad (5)$$

$$\|\mathbf{z} + \delta_z - \mathbf{z}\| \leq K \cdot \|\delta\| \quad (6)$$

$$\|\delta_z\| \leq K \cdot c \quad (7)$$

Proposition 1 indicates that If $0 < K < 1$, δ_z will be at least $\frac{1}{K}$ times smaller than δ . Hence, the induced perturbation in the latent space can be made as small as possible by controlling K . Further, even in absence of adversarial examples, a defense strategy can be devised by randomly sampling a latent vector $\hat{\mathbf{z}}$ from $[\mathbf{z}, \mathbf{z} + \delta_z]$, generating a data sample from it and filtering out δ_z . Since the goal is to learn mappings in high-dimensional spaces, we use Deep-neural networks (DNN) parameterized by θ , to approximate f_θ . There have been many methods proposed to make a DNN K -Lipschitz including gradient clipping [1] and gradient norm penalty [12]. We employ gradient norm penalty on every batch B of encoder training since it is observed to be more stable, given by following:

$$\mathcal{L}_l = \sum_{i=1}^B \left(\left\| \nabla_x f_\theta(x^{(i)}) \right\|_2 - K \right)^2 \quad (8)$$

where K is the Lipschitz constant.

3.3. Latent exploration via variational inference

As mentioned earlier, the goal is to explore the latent neighbourhood induced by perturbing a given input sam-

ple. This effectively means that one has to sample from the true conditional distribution $p(\mathbf{z}|\mathbf{x})$. However since there is no direct access to $p(\mathbf{z}|\mathbf{x})$ we propose to use the principles of variational inference [15], where sampling from $p(\mathbf{z}|\mathbf{x})$ is facilitated by reducing the distance between $p(\mathbf{z}|\mathbf{x})$ and an arbitrary variational distribution $q(\mathbf{z}|\mathbf{x})$ on \mathbf{z} that is parameterized by the encoder network f_θ . Now minimizing the KL-divergence between $p(\mathbf{z}|\mathbf{x})$ and $q(\mathbf{z}|\mathbf{x})$ results in the maximization of the so-called evidence lower bound given as follows:

$$\mathcal{L} = \mathbb{E}_{q_\theta(\mathbf{z}|\mathbf{x})}[\ln(p_\phi(\mathbf{x}|\mathbf{z}))] - \mathbb{D}_{KL}(q_\theta(\mathbf{z}|\mathbf{x})||p_\theta(\mathbf{z})) \quad (9)$$

where $p_\phi(\mathbf{x}|\mathbf{z})$ represents a probabilistic decoder network that maps the latent space back to the data space and $p_\theta(\mathbf{z})$ is an arbitrary prior on \mathbf{z} which is usually a Normal distribution. We propose to sample $\hat{\mathbf{z}}$ from $q_\theta(\mathbf{z}|\mathbf{x})$ using the encoder network f_θ through the reparameterization trick [15]. Thus, given a true data example, a cloud of perturbations is created around its latent representation obtained through Lipschitz constrained encoder f_θ , via variational sampling. The probabilistic decoder $p_\phi(\mathbf{z})$, parameterized using a neural network g_ϕ , is then tasked to map all the points within that cloud to a single input example through maximization of the likelihood term in equation 9, as shown in Figure 1. Mathematically, if encoder embeds an $\mathbf{x} + \delta$ to a $\hat{\mathbf{z}}$, such that $\|\hat{\mathbf{z}} - \mathbf{z}\| \leq \delta_z$ then decoder learns $g_\phi(\hat{\mathbf{z}}) = \mathbf{x}$. During inference, When the encoder is presented with an adversarial example, it will place it within the learned latent cloud so that the decoder converts into a non-adversarial sample.

This fact has been illustrated in Figure 2 where a 2D t-SNE plot of the latent encodings (from the Lipschitz constrained encoder) of the true and the CW l_2 attacked adversarial samples from the MNIST data is shown. It can be seen that embeddings of the adversaries are extremely close to those of true samples.

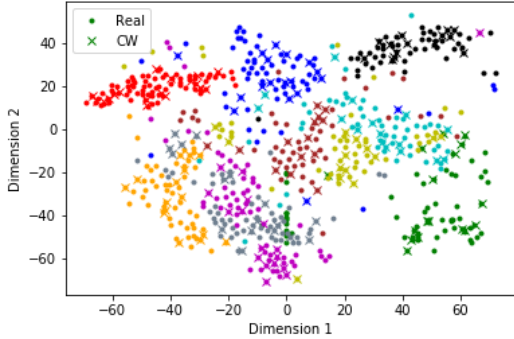


Figure 2. t-SNE plot of the latent encodings of mnist real images and CW adversarial images. It can be seen that the embeddings of real and adversarial data overlap.

3.4. Latent space quantization

A recent work by Gilmer et.al[7] makes a very important observation - closeness from a correctly classified sample does not guarantee non-adversarial nature. In other words, since the latent space is real-valued it is impossible to explore it in its entirety. Thus, there is a high chance that a probabilistic decoder g_ϕ is unable to remove the adversarial noise even when the latent vector for an adversarial example falls within the seen latent cloud. We propose to address this issue by quantizing the latent space before it is input to the decoder. Specifically, we design a fixed discrete quantization function H applied on each dimension of the real-output of the encoder as follows:

$$H_i(\hat{z}) = \begin{cases} +1 & \text{if } \|\hat{z}_i\| \leq \eta_{zi} \\ -1 & \text{otherwise} \end{cases} \quad (10)$$

where η_z is the quantization threshold. For simplicity we assume all η_{zi} 's to be equal. $H(\cdot)$ thus converts \hat{z} into binary coded vectors thereby ensuring that the decoder g_ϕ receives a single latent code for all the input samples that map within the latent cloud with \hat{z} with $\|\hat{z}\| \leq \eta_z$. In contrast to real \hat{z} , where g_ϕ has to learn a non-injective mapping, quantization allows it to learn a mapping close to injective since a same code vector is produce for all \hat{z} with $\|\hat{z}\| \leq \eta_z$, hence making the training easier. This procedure potentially increases the robustness of the model too since the goal of a adversarial resilience model is not to exactly reproduce the non-adversarial version of a given sample but to produce an approximate version that is non-adversarial. Thus, it is imperative to just look for the presence or absence of

the salient features that preserves the identity of a given example, which is accomplished by the binary quantization with the threshold η_z being a hyperparameter whose value is used as, however not limited to, $2 \times \delta_z/3$. Thus, any deviation in the input sample falling outside the latent cloud leads to flipping of the bits in the quantized space. Figure 3 depicts the bit-flippings in the latent codes of the CW adversaries on the MNIST data - It can be seen that about 90 % of the total adversaries undergo less than 6% of the bit flipping high classification accuracy, confirming the effectiveness of the decoder in ignoring the bit-flippings. Further, the binary encoding offers layer ensures that gradient produced at that layer is either 0 or undefined, thereby making a gradient based attack on the defense impossible.

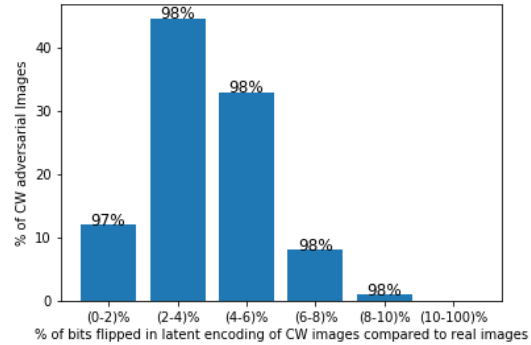


Figure 3. Effect of binary quantization on adversaries - It can be seen that more than 90 % of the adversaries have less than 6% of the bit flippings with high classification accuracy.

3.5. Adversarial resilience by LQ-VAE

As mentioned above, quantization prevents the flow of gradients through the encoder network f_θ that makes it non-trainable along with the decoder g_ϕ . We, therefore, create a copy of g_ϕ , say h_ψ , which uses soft quantization in place of H (called the \tilde{H}) and enable the training of f_θ . A complete overview of the proposed method, called as Lipschitz-constrained quantized variational auto-encoder (LQ-VAE) is shown in Figure 1. Algorithm 1 gives the details of the LQ-VAE training procedure where the likelihood term in equation 9 is approximated using an mean-squared error term between the input and the output. Note that the network h_ψ is only used for training, not for inference. The defense scheme only contains the pipeline of $f_\theta - H - g_\phi$.

4. Experiments and results

We consider MNIST [18], FMNIST¹, and CelebA [20] datasets and use three classifier architectures, named A, B, and C, for black box and white box experiments². For

¹<https://github.com/zalando-research/fashion-mnist>

²Architectures of all the classifiers and LQ-VAE is included in supplementary material.

Algorithm 1 LQ-VAE algorithm

Input: Dataset \mathcal{D} , Batchsize B , Encoder f_θ , Decoder g_ϕ , Learning rate η , Quantization functions H, \tilde{H}
Output Parameters θ^*, ϕ^*

- 1: Make a copy h_ψ of decoder g_ϕ
 - 2: **repeat**
 - 3: Sample $\{\mathbf{x}^{(1)} \dots \mathbf{x}^{(B)}\}$ from dataset \mathcal{D}
 - 4: $\mu_{\mathbf{z}}^{(i)}, \sigma_{\mathbf{z}}^{(i)} \leftarrow f_\theta(\mathbf{x}^{(i)})$
 - 5: Sample $\hat{\mathbf{z}}^{(i)}$ from $\mathcal{N}(\mu_{\mathbf{z}}^{(i)}, \sigma_{\mathbf{z}}^{(i)2})$
 - 6: $\hat{\mathbf{x}}_1^{(i)} \leftarrow h_\psi(\tilde{H}(\hat{\mathbf{z}}^{(i)}))$
 - 7: $\hat{\mathbf{x}}_2^{(i)} \leftarrow g_\phi(H(\hat{\mathbf{z}}^{(i)}))$
 - 8: $\mathcal{L}_h \leftarrow \sum_{i=1}^B \left\| \mathbf{x}^{(i)} - \hat{\mathbf{x}}_1^{(i)} \right\|_2^2$
 - 9: $\mathcal{L}_g \leftarrow \sum_{i=1}^B \left\| \mathbf{x}^{(i)} - \hat{\mathbf{x}}_2^{(i)} \right\|_2^2$
 - 10: $\mathcal{L}_f \leftarrow \mathcal{L}_h + \sum_{i=1}^B \mathbb{D}_{KL}(\mathcal{N}(\mu_{\mathbf{z}}^{(i)}, \sigma_{\mathbf{z}}^{(i)2}) \parallel \mathcal{N}(0, 1)) + \sum_{i=1}^B (\left\| \nabla_x f_\theta(x^{(i)}) \right\|_2 - K)^2$
 - 11: $\theta \leftarrow \theta + \eta \nabla_\theta \mathcal{L}_f$
 - 12: $\phi \leftarrow \phi + \eta \nabla_\phi \mathcal{L}_g$
 - 13: $\psi \leftarrow \psi + \eta \nabla_\psi \mathcal{L}_h$
 - 14: **until** convergence of θ, ϕ
-

MNIST and FMNIST, the standard 10 class classification task is considered, whereas for CelebA, a binary classification task is of gender classification is taken, with accuracy as the metric. Five attack types namely, FGSM with $\epsilon = 0.3$ [10], l_2 CW [4], Deepfool [25], iterative FGSM [16] and Madry [21], generated from cleverhans library [26], are considered for experimentation as they cover good breadth of attack types. We compare our results with three defense strategies - Defense GAN [30], Madry [21] and Adversarial retraining [10] based on the following facts (i) Defense GAN is close to our work in spirit. Their method also employs a generative model (GAN) and does not train on adversarial examples, (ii) Madry retraining is claimed to be a robust defense against all first-order gradient computation based attacks and (iii) adversarial retraining is the one of the earliest benchmark defense created. Further, we study the effect of the quantization hyperparameter δ_z on the performance. Finally, we conduct ablation studies on our method by removing the quantization and Lipschitz constraints on LQ-VAE. We use Adam optimizer ($\beta_1 = 0.9, \beta_2 = 0.99$) with learning rate of $\times 10^{-3}$ to train LQ-VAE.

4.1. Results on white box attacks

For MNIST and FMNIST, we use 60,000 real images for training of the defense mechanisms and 10,000 adversarial images on the standard test set for testing. For CelebA, we use 90% images for training and remaining for testing. Classification accuracy of all three classifier models, A, B, and C, in presence and absence of defense mechanisms

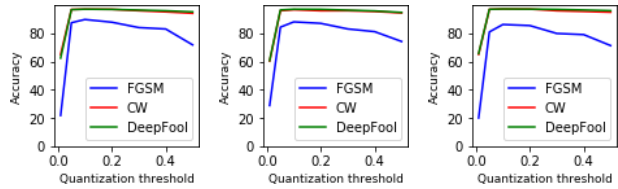


Figure 4. Effect of LQ-VAE quantization threshold variation on the classification accuracy of the model A (left), B (middle), and C (right).

are listed in Table 1, 2, and 3 for MNIST, FMNIST, and CelebA, respectively. The attacks reduce classification accuracy of all the models drastically. Adversarial retraining is able to defend FGSM attack up to a certain extent but fails on the other attacks, since the retraining is performed using adversarial examples generated by FGSM attacks. Similarly Madry, which also uses first order gradients based adversarial images to retrain the classifiers, shows consistent performance against FGSM. However, for Deepfool and CW attack, its performance is lower than Defense-GAN and the proposed LQ-VAE. Both, Defense-GAN and LQ-VAE, do not require adversarial augmentation, however, we note that LQ-VAE consistently outperforms the Defense-GAN. We assume complete knowledge of classifier as well as defense mechanism for attack, however, quantization of latent space prevents further attacks on LQ-VAE.

4.2. Results on black box attacks

For black box experiments, we consider one attack each on a dataset as a representative set. Specifically, FGSM for MNIST, Deepfool for FMNIST and CW for CelebA are considered with six-pairs of classifiers used for attacking and substitute. A similar trend is observed with the black box attacks as well, as seen in Tables 4, 5 and 6. Madry retraining performs the best on the FGSM attack because it is trained on a superset of first-order methods of which FGSM is a subset. However, the performance of LQ-VAE is consistent irrespective of the classifier pairs across all cases and is closely comparable (or better) to the best case. On Deepfool and CW, LQ-VAE outperforms the others in most of the cases. We hypothesize that this behaviour of LQ-VAE comes from the Lipschitz constraining, by which it becomes a strong defense when the attack alters fewer pixels of the input image yet changing the class, as in the case of CW and Deepfool, unlike in FGSM. In summary, the proposed method is invariant to white or black box attack types.

4.3. Effect of the parameter δ_z

The quantization step, key factor behind the better performance of LQ-VAE, is closely related to the assumed perturbation limit δ_z . We, therefore, vary δ_z and accordingly adjust the quantization threshold to measure the accuracy of different models for FGSM attacks on MNIST. The ob-

Attack	Model	No Attack	No Defense	LQ-VAE	Defense-GAN	Madry	Adv Tr
FGSM	A	99.40	20.16	89.17	90.43	96.85	67.95
	B	99.41	13.17	86.70	88.52	96.20	49.49
	C	98.37	5.66	83.02	86.7	84.71	80.75
Deepfool	A	99.40	7.38	97.60	95.41	67.82	3.10
	B	99.41	5.88	97.74	93.03	66.35	5.75
	C	98.37	48.24	97.42	92.32	62.38	10.97
CW	A	99.40	8.85	97.66	94.37	69.15	1.20
	B	99.41	5.07	97.20	90.56	71.35	1.45
	C	98.37	8.44	97.36	92.5	58.65	2.15

Table 1. Classification accuracy of the MNIST classifiers on white box attacks with various defense strategies.

Attack	Model	No Attack	No Defense	LQ-VAE	Defense-GAN	Madry	Adv Tr
FGSM	A	92.76	11.5	77.0	69.75	78.87	53.72
	B	91.17	10.14	69.41	56.72	76.94	59.79
	C	89.06	11.6	67.07	56.34	64.16	66.43
Deepfool	A	92.76	5.29	79.3	77.48	57.17	6.52
	B	91.17	6.54	79.41	74.97	52.58	14.74
	C	89.06	7.65	79.89	74.82	39.93	24.71
CW	A	92.76	5.41	80.64	78.75	62.55	5.35
	B	91.17	6.61	81.58	78.18	56.48	6.35
	C	89.06	7.89	82.31	78.58	43.72	8.00

Table 2. Classification accuracy of the FMNIST classifiers on white box attacks with various defense strategies

Attack	Model	No Attack	No Defense	LQ-VAE	Defense-GAN	Madry	Adv Tr
FGSM	A	96.34	3.65	81.04	74.13	62.35	4.53
	B	96.60	3.40	64.74	67.06	71.42	72.88
	C	95.02	28.62	61.48	53.76	61.35	42.55
Deepfool	A	96.34	3.56	85.89	83.87	52.86	6.26
	B	96.60	2.43	83.81	83.65	49.39	14.17
	C	95.02	10.92	62.79	78.56	42.37	38.45
CW	A	96.34	6.98	85.90	84.64	58.62	11.88
	B	96.60	6.88	86.29	86.01	60.33	12.91
	C	95.02	10.92	79.20	78.56	45.02	38.45
Iter FGSM	A	96.34	3.12	85.44	81.00	82.34	3.50
	B	96.60	3.55	72.29	72.05	72.19	9.16
	C	95.02	11.92	52.12	42.13	90.87	19.47
Madry	A	96.34	2.84	85.11	81.43	76.35	3.52
	B	96.60	3.12	70.01	74.01	70.32	8.52
	C	95.02	8.57	54.00	45.11	84.09	18.59

Table 3. Classification accuracy of the CelebA classifiers on white box attacks with various defense strategies.

servations are plotted in Figure 4. The best performance of all the classifiers is observed for quantization threshold of 0.1 or $\delta_z = 0.15$. The smaller δ_z is insufficient for the perturbations occurring due to FGSM, whereas larger δ_z make the perturbation clouds of different samples overlap, resulting in an imprecise convergence of the decoder g_ϕ . Thus $\delta_z = 0.15$ sets a trade-off between acceptable perturbation limit and convergence of g_ϕ .

4.4. Ablation on LQ-VAE

To study the extent of usefulness of the Lipschitz constraint and latent quantization, we conduct ablation in this section using MNIST dataset for white box FGSM attack which exposes the vulnerability of the defense strategy. Without Lipschitz constraint and latent quantization, LQ-VAE becomes a conventional VAE. The results of this experiment are shown in Table 7. It can be seen that in

Classifier Substitute	No Attack	No Defense	LQ-VAE	Defense-GAN	Madry	Adv Tr
A/B	99.4	33.32	88.09	89.14	97.17	95.78
A/C	99.4	45.35	90.60	90.08	98.27	96.82
B/A	99.41	42.22	90.63	91.4	97.38	94.64
B/C	99.41	38.73	89.92	89.89	98.03	95.3
C/A	98.37	28.93	91.98	90.9	90.59	32.12
C/B	98.37	18.01	89.38	88.73	89.14	21.79

Table 4. Classification accuracy of the MNIST classifier on FGSM black box attack images generated using substitute model.

Classifier/ Substitute	No Attack	No Defense	LQ-VAE	Defense-GAN	Madry	Adv Tr
A/B	92.76	29.14	77.74	74.41	60.11	48.27
A/C	92.76	35.44	77.11	74.11	62.58	57.53
B/A	91.17	67.82	81.33	77.97	80.71	76.61
B/C	91.17	45.55	78.83	74.5	69.19	64.05
C/A	89.06	79.11	82.12	78.82	80.99	81.84
C/B	89.06	47.26	80.76	76.6	67.46	59.64

Table 5. Classification accuracy of the FMNIST classifier on Deepfool black box attack images generated using substitute model.

Classifier/ Substitute	No Attack	No Defense	LQ-VAE	Defense-GAN	Madry	Adv Tr
A/B	96.34	39.53	86.01	84.7	85.41	94.13
A/C	96.34	37.59	80.10	78.11	64.72	54.22
B/A	96.60	49.21	85.67	86.19	82.55	68.11
B/C	96.60	52.52	79.98	79.91	76.31	62.53

Table 6. classification accuracy of the CelebA classifier on CW black box attack images generated using substitute model

Model	No Attack	No Defense	VAE	LQ-VAE
A	99.40	20.16	50.10	89.17
B	99.41	13.17	67.37	86.70
C	98.37	5.66	49.18	83.02

Table 7. Classification accuracy of whitebox FGSM attack on Model-VAE and Model-LQ-VAE pipeline(MNIST).

presence of conventional VAE defense, FGSM exploits the backpropagation path to attack the whole pipeline of classifier and VAE, however, only a limited amount of defense is achieved whereas in contrast, the defense produced by the LQ-VAE is considerably better.

4.5. Discussions and Conclusions

LQ-VAE and Defense GAN fall into the same category of defense mechanism in that they both capitalize on the expressive capacity of generative models. Further, both of the models generalize better on the adaptive or unseen attacks [2] since both of them neither need access to the classifier nor train on a certain type of adversaries. However, LQ-VAE offers several advantages over the Defense-GAN such as - (i) LQ-VAE does not involve a run-time search on the latent space unlike Defense-GAN which makes it orders of magnitude faster and independent of latent search parameters.

Rather in LQ-VAE, the search in the latent space is implicitly done by effective encoding, quantization and decoding of the latent space. (ii) training a VAE is known to be easier and faster yielding a better data likelihood than a GAN which is known to be difficult to be trained, especially on color datasets such as CelebA, (iii) LQ-VAE has a latent encoding followed by the re-mapping of the latent space to the data space which makes its invariant to attack types while Defense-GAN is shown to degrade in the case of black box, (iv) as argued in [2], Defense-GAN can be attacked too by a method called the Backward Pass Differentiable approximation, in which case its defense on MNIST is reported at 55 % [2]. When the same technique is used to attack LQ-VAE, we obtained an accuracy of 60 % on the same task which can be ascribed to use of latent space constraining and quantization. In summary, we proposed a technique called the LQ-VAE as a filter for the adversarial resilience using a constrained projection on to a quantized latent space followed by data reconstruction. It serves like a ‘black-box defense’ in the sense that it can be used to defend any attack and with any classifier. In principle, LQ-VAE can be re-trained using adversaries too, in which case the performance is observed to improve. For instance, it is observed that if one retrains LQ-VAE using Madry adversaries, its

performance is enhanced by 5-10 % on FGSM attacks. Future directions include exploration of the latent prior p_θ beyond a standard Normal distribution, studying the effect of different types of quantization other than a simple binary quantization, using LQ-VAE as an adversarial detector.

References

- [1] M. Arjovsky, S. Chintala, and L. Bottou. Wasserstein gan. *arXiv preprint arXiv:1701.07875*, 2017. 4
- [2] A. Athalye, N. Carlini, and D. Wagner. Obfuscated gradients give a false sense of security: Circumventing defenses to adversarial examples. *arXiv preprint arXiv:1802.00420*, 2018. 3, 8
- [3] N. Carlini and D. Wagner. Towards Evaluating the Robustness of Neural Networks. *arXiv e-prints*, page arXiv:1608.04644, Aug. 2016. 2
- [4] N. Carlini and D. Wagner. Towards evaluating the robustness of neural networks. In *2017 IEEE Symposium on Security and Privacy (SP)*, pages 39–57. IEEE, 2017. 1, 2, 6
- [5] G. S. Dhillon, K. Aizzadenesheli, Z. C. Lipton, J. Bernstein, J. Kossaifi, A. Khanna, and A. Anandkumar. Stochastic activation pruning for robust adversarial defense. *arXiv preprint arXiv:1803.01442*, 2018. 3
- [6] G. W. Ding, K. Y. C. Lui, X. Jin, L. Wang, and R. Huang. On the sensitivity of adversarial robustness to input data distributions. *arXiv preprint arXiv:1902.08336*, 2019. 2
- [7] J. Gilmer, L. Metz, F. Faghri, S. S. Schoenholz, M. Raghu, M. Wattenberg, and I. Goodfellow. Adversarial spheres. *arXiv preprint arXiv:1801.02774*, 2018. 1, 3, 5
- [8] I. Goodfellow, Y. Bengio, A. Courville, and Y. Bengio. *Deep learning*, volume 1. MIT Press, 2016. 2
- [9] I. Goodfellow, J. Pouget-Abadie, M. Mirza, B. Xu, D. Warde-Farley, S. Ozair, A. Courville, and Y. Bengio. Generative adversarial nets. In *Advances in neural information processing systems*, pages 2672–2680, 2014. 3
- [10] I. J. Goodfellow, J. Shlens, and C. Szegedy. Explaining and harnessing adversarial examples. *arXiv preprint arXiv:1412.6572*, 2014. 1, 2, 6
- [11] I. J. Goodfellow, J. Shlens, and C. Szegedy. Explaining and Harnessing Adversarial Examples. *arXiv e-prints*, page arXiv:1412.6572, Dec. 2014. 2
- [12] I. Gulrajani, F. Ahmed, M. Arjovsky, V. Dumoulin, and A. C. Courville. Improved training of wasserstein gans. In *Advances in Neural Information Processing Systems*, pages 5767–5777, 2017. 4
- [13] C. Guo, M. Rana, M. Cisse, and L. van der Maaten. Countering adversarial images using input transformations. *arXiv preprint arXiv:1711.00117*, 2017. 3
- [14] A. Ilyas, A. Jalal, E. Asteri, C. Daskalakis, and A. G. Dimakis. The robust manifold defense: Adversarial training using generative models. *arXiv preprint arXiv:1712.09196*, 2017. 2
- [15] D. P. Kingma and M. Welling. Auto-encoding variational bayes. *arXiv preprint arXiv:1312.6114*, 2013. 4
- [16] A. Kurakin, I. Goodfellow, and S. Bengio. Adversarial examples in the physical world. *arXiv preprint arXiv:1607.02533*, 2016. 2, 6
- [17] A. Kurakin, I. J. Goodfellow, and S. Bengio. Adversarial machine learning at scale. *CoRR*, abs/1611.01236, 2016. 2
- [18] Y. LeCun, C. Cortes, and C. Burges. Mnist handwritten digit database. *AT&T Labs [Online]*. Available: <http://yann.lecun.com/exdb/mnist>, 2, 2010. 5
- [19] H. Lee, S. Han, and J. Lee. Generative adversarial trainer: Defense to adversarial perturbations with gan. *arXiv preprint arXiv:1705.03387*, 2017. 3
- [20] Z. Liu, P. Luo, X. Wang, and X. Tang. Deep learning face attributes in the wild. In *Proceedings of the IEEE International Conference on Computer Vision*, pages 3730–3738, 2015. 5
- [21] A. Madry, A. Makelov, L. Schmidt, D. Tsipras, and A. Vladu. Towards deep learning models resistant to adversarial attacks. *arXiv preprint arXiv:1706.06083*, 2017. 1, 2, 6
- [22] A. Madry, A. Makelov, L. Schmidt, D. Tsipras, and A. Vladu. Towards Deep Learning Models Resistant to Adversarial Attacks. *arXiv e-prints*, page arXiv:1706.06083, June 2017. 2
- [23] D. Meng and H. Chen. Magnet: a two-pronged defense against adversarial examples. In *Proceedings of the 2017 ACM SIGSAC Conference on Computer and Communications Security*, pages 135–147. ACM, 2017. 2, 3
- [24] S. Moosavi-Dezfooli, A. Fawzi, and P. Frossard. Deepfool: a simple and accurate method to fool deep neural networks. *CoRR*, abs/1511.04599, 2015. 2
- [25] S.-M. Moosavi-Dezfooli, A. Fawzi, and P. Frossard. Deepfool: a simple and accurate method to fool deep neural networks. In *Proceedings of the IEEE Conference on Computer Vision and Pattern Recognition*, pages 2574–2582, 2016. 1, 2, 6
- [26] N. Papernot, I. Goodfellow, R. Sheatsley, R. Feinman, and P. McDaniel. cleverhans v1.0.0: an adversarial machine learning library. *arXiv preprint arXiv:1610.00768*, 2016. 6

- [27] N. Papernot, P. McDaniel, I. Goodfellow, S. Jha, Z. B. Celik, and A. Swami. Practical black-box attacks against machine learning. In *Proceedings of the 2017 ACM on Asia Conference on Computer and Communications Security*, pages 506–519. ACM, 2017. [1](#)
- [28] N. Papernot, P. McDaniel, S. Jha, M. Fredrikson, Z. B. Celik, and A. Swami. The limitations of deep learning in adversarial settings. In *2016 IEEE European Symposium on Security and Privacy (EuroS&P)*, pages 372–387. IEEE, 2016. [2](#)
- [29] N. Papernot, P. McDaniel, X. Wu, S. Jha, and A. Swami. Distillation as a defense to adversarial perturbations against deep neural networks. In *2016 IEEE Symposium on Security and Privacy (SP)*, pages 582–597. IEEE, 2016. [2](#)
- [30] P. Samangouei, M. Kabkab, and R. Chellappa. Defense-gan: Protecting classifiers against adversarial attacks using generative models, 2018. [2](#), [3](#), [6](#)
- [31] L. Schmidt, S. Santurkar, D. Tsipras, K. Talwar, and A. Madry. Adversarially robust generalization requires more data. In *Advances in Neural Information Processing Systems*, pages 5019–5031, 2018. [1](#)
- [32] Y. Sharma and P.-Y. Chen. Attacking the madry defense model with l_1 -based adversarial examples. *arXiv preprint arXiv:1710.10733*, 2017. [2](#)
- [33] S. Shen, G. Jin, K. Gao, and Y. Zhang. Ape-gan: Adversarial perturbation elimination with gan. *arXiv preprint arXiv:1707.05474*, 2017. [2](#), [3](#)
- [34] A. Sinha, H. Namkoong, and J. Duchi. Certifying some distributional robustness with principled adversarial training. *arXiv preprint arXiv:1710.10571*, 2017. [2](#)
- [35] Y. Song, T. Kim, S. Nowozin, S. Ermon, and N. Kushman. Pixeldefend: Leveraging generative models to understand and defend against adversarial examples. *arXiv preprint arXiv:1710.10766*, 2017. [2](#), [3](#)
- [36] C. Szegedy, W. Zaremba, I. Sutskever, J. Bruna, D. Erhan, I. Goodfellow, and R. Fergus. Intriguing properties of neural networks. *arXiv preprint arXiv:1312.6199*, 2013. [1](#), [2](#)
- [37] F. Tramèr, A. Kurakin, N. Papernot, I. Goodfellow, D. Boneh, and P. McDaniel. Ensemble adversarial training: Attacks and defenses. *arXiv preprint arXiv:1705.07204*, 2017. [2](#)
- [38] D. Tsipras, S. Santurkar, L. Engstrom, A. Turner, and A. Madry. Robustness may be at odds with accuracy. *stat*, 1050:11, 2018. [1](#)
- [39] K. Y. Xiao, V. Tjeng, N. M. Shafiullah, and A. Madry. Training for faster adversarial robustness verification via inducing relu stability. *arXiv preprint arXiv:1809.03008*, 2018. [3](#)
- [40] C. Xie, J. Wang, Z. Zhang, Z. Ren, and A. Yuille. Mitigating adversarial effects through randomization. *arXiv preprint arXiv:1711.01991*, 2017. [3](#)